Model Independence, Dispersion Approach and Nucleon Form-Factors

Krzysztof M. Graczyk

Instytut Fizyki Teoretycznej
Uniwersytet Wrocławski
Polska

Seminar of Neutrino Physics Division

3d November 2014, Wrocław

- Model Independent Extraction of the Proton Radius:
  - Electric: R. J. Hill and G. Paz, PRD82, 113005 (2010)
  - Magnetic: Z. Epstein, G. Paz, J. Roy, Phys.Rev. D90 (2014) 074027
- Axial mass problem:
  - R J. Hill and G. Paz, PRD84, 073006 (2011)
- Model Independence in the Statistical Sense
  - K. M. Graczyk, C. Juszczak, arXiv:1408.0150

- Model Independent Extraction of the Axial Form Factor, Axial Radius?
- Recent M_A measurements ~ 1.3 GeV old 1.0 GeV

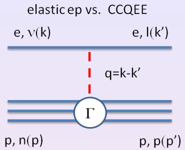

$$\mathcal{M}^{ep}_{Born} = -i\frac{e^2}{q^2}\bar{u}(k')\gamma_\mu u(k)\, h^\mu_{ep}$$

$$i\mathcal{M}^{\nu n}_{Born} \approx i\frac{g^2\cos\theta_C}{8(q^2-M_W^2)}\overline{u}(k')\gamma_\mu(1-\gamma_5)u(k)\, h^\mu_{cc}$$

$$h^\mu_{ep/\nu n} = \overline{u}(p')\Gamma^\mu_{p,W}(q)u(p) \quad Q^2 = -q^2 = -t$$

After **CVC** and **PCAC**

$$\Gamma^\mu_W = \underbrace{\Gamma^\mu_p(q) - \Gamma^\mu_n(q)}_{vector} - \underbrace{\gamma_\mu\gamma_5 F_A(q) - \frac{q^\mu\gamma_5}{2M}F_P(q)}_{axial},$$

$$F_A(q) = \frac{1.267}{(1-q^2/M_A^2)^2}$$

$$F_P(q) = \frac{4M^2F_A(q)}{m_\pi^2 - q^2}$$

$$\Gamma^\mu_N = \gamma^\mu F_1^N(Q^2) + \frac{i\sigma^{\mu\nu}q_\nu}{2M_p}F_2^N(Q^2),$$

$$N = \mathbf{proton},\ \mathbf{neutron}$$

$$F_1(Q^2) = \frac{1}{1+\tau}\left(G_E(Q^2) + \tau G_M(Q^2)\right)$$

$$F_2(Q^2) = \frac{1}{1+\tau}\left(G_M(Q^2) - G_E(Q^2)\right)$$

$\tau = Q^2/4M^2$ electric, magnetic

Axial mass M_A problem: ν-deuteron scattering data ($\sim$ 1 GeV), ν-Carbon $\sim$ 1.3 GeV ? Need of more sophisticated nuclear models?

- Model Independent Extraction of the Proton Radius?

$$\rho_{E,M}(r) = \frac{1}{(2\pi)^3}\int d^3q e^{-i\mathbf{q}\cdot r} G_{E,M}(\mathbf{q})$$

$$\left\langle r^2_{E,M} \right\rangle = -6\frac{dG_{E,M}(\mathbf{q})}{d|\mathbf{q}|^2}\bigg|_{|\mathbf{q}|^2=0}$$

$$G_{E,M}(Q^2) = G_{E,M}(0) - \frac{1}{6}\left\langle r^2_{E,M}\right\rangle Q^2 + \ldots$$

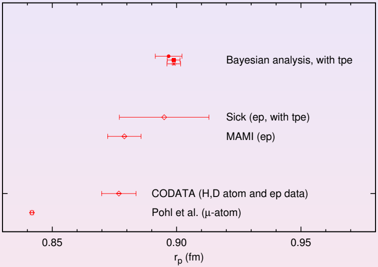

RICHARD J. HILL AND GIL PAZ PHYSICAL REVIEW D **82,** 113005 (2010)

TABLE I. Proton charge radius extracted from data of Table 1 of [18] ($Q^2 \lesssim 0.04$ GeV^2) in units of 10^{-18} m, using different functional behaviors of the form factor. Dots denote fits that do not constrain the slope to be positive.

	$k_{max} = 1$	2	3	4	5
Polynomial	836^{+8}_{-9}	867^{+23}_{-24}	866^{+52}_{-56}	959^{+85}_{-93}	1122^{+122}_{-137}
	$\chi^2 = 34.49$	32.51	32.51	31.10	28.99
Continued fraction	882^{+10}_{-10}	869^{+26}_{-25}	...	...	...
	$\chi^2 = 32.81$	32.51			
z expansion (no bound)	918^{+9}_{-9}	868^{+28}_{-29}	879^{+64}_{-69}	1022^{+102}_{-114}	1193^{+152}_{-174}
	$\chi^2 = 36.14$	32.52	32.48	30.35	28.92
z expansion ($\lvert a_k \rvert \leq 10$)	918^{+9}_{-9}	868^{+28}_{-29}	879^{+38}_{-59}	880^{+39}_{-61}	880^{+39}_{-62}
	$\chi^2 = 36.14$	32.52	32.48	32.46	32.45

S-matrix theory $\rightarrow$ Hadron Physics

- Lorentz invariance of the theory and other symmetry principles
- unitarity of the S-matrix
- anlyticity
  - scattering amplitudes, when expressed as functions of certain kinematic variables, can be analytically continued into the complex domain and resulting analytic functions, at least near the physical regions, have the simplest singularity structure which is consistent with the other general principles of the theory
- crossing

Analytic Function

Single-valued function of z is said to be analytic at point z_0 if it has a derivative at z_0 and at all points in some neighbourhood z_0.
If function is not analytic at point z_0 we say it is singular there.

Property

All derivatives of an analytic function are analytic.

Cauchy's theorem

If the function f(z) is analytic through the region enclosed by the closed contour C in the complex z-plane then

$$\oint_C f(z)dz = 0$$

The residue theorem

If f(z) has no singularities other then poles in the interior of the closed contour C, then

$$\oint_C f(z)dz = 2\pi i R$$

where R is the sum of residues of these poles and the integration is taken in anticlockwise sense.

Cauchy's integral formula

If $f(z)$ is analytic through the interior of the closed contour C, then at any interior point z of this region,

$$f(z) = \frac{1}{2\pi i} \oint_C \frac{f(z')}{z' - z} dz'$$

The Schwarz reflection principle

If $f(z)$ is analytic in a connected region which includes part of the real axis and $f(z)$ is real-valued on this part of the real axis, then

$$f(z^*) = f^*(z)$$

Laurent's theorem

Let f(z) be analytic through the closed annular region between the two circles C_1 and C_2 with common centre z_0. Then at each point in this annulus

$$f(z) = \sum_{n=-\infty}^{\infty} A_n (z - z_0)^n,$$

with series converging uniformly in any closed region, R, lying wholly within the annulus. Here

$$A_n = \frac{1}{2\pi i} \oint_C \frac{f(z')}{(z' - z_0)^{n+1}} dz'$$

Taylor's Theorem

If $f(z)$ is analytic at all points interior to a circle C centered about z_0 then in any closed region contained wholly inside C

$$f(z) = \sum_{n=0}^{\infty} \frac{1}{n!} f^{(n)}(z_0)(z - z)0)^n$$

and the series converges uniformly.

Casuality

In non-relativistic physics the recruitment of causality follows the analyticity of the $f(E)$ scattering amplitude in the upper half-plane of the complex plane (in E).

see (Bjorken & Drell, 1998)

Electromagnetic Vertex

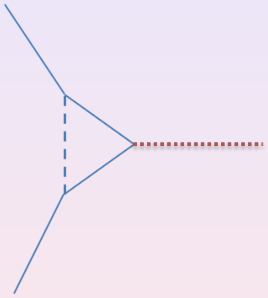

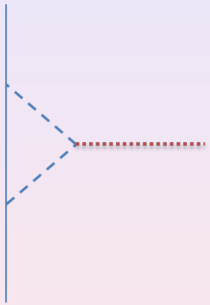

Electromagnetic Vertex

$$F(q^2) \sim \int d^4k \frac{1}{(k^2 - m_\pi^2 + i\epsilon)((k+q)^2 - m_\pi^2 + i\epsilon)((p-k)^2 - M^2) + i\epsilon)}$$

We easily get,

$$F(q^2) \sim \int_0^1 dx \int_0^{1-x} dy \int d^4k' \frac{1}{[k'^2 + \Delta + i\epsilon]^3}$$

where

$$\Delta = q^2xy - M^2(x+y-1)^2 - m^2(x+y) + i\epsilon \to \Delta = (q^2xy + i\epsilon') - M^2(x+y-1)^2 - m^2(x+y) \quad (1)$$

In practise,

$$F(q^2 + i\epsilon') \sim \int_0^1 dx \int_0^{1-x} dy \frac{1}{[\Delta]}$$

It is easy to see that Δ vanishes along $q^2 > 4m_\pi$! Hence $F(z)$ is analytic in complex plane but without cut along Rez axis starting from $z = 4m_\pi$

- $q^2 = t$, for elastic scattering $t < 0$!
- Large distance from singularities implies the existence of the expansion parameter
- Conformal Mapping on unit circle

$$z(t) = \frac{\sqrt{t_{cut} - t} - \sqrt{t_{cut} - t_0}}{\sqrt{t_{cut} - t} + \sqrt{t_{cut} + t_0}}$$

$$t_{cut} = 4m_\pi^2,$$
$$t_0 = t_{cut}(1 - \sqrt{1 + Q_{max}^2/t_{cut}})$$

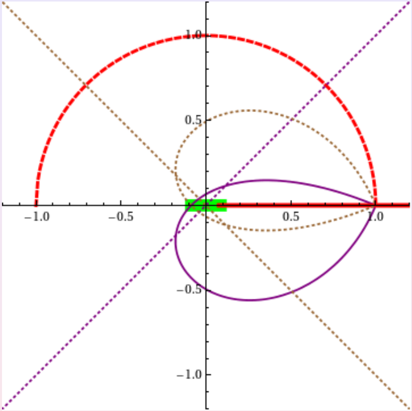

Notice that

$$\lim_{|t|\to\infty} z(t) = 1$$

as well as

$$z(t=-Q^2_{max}) = -z(t=0) = z_{max}$$

Line segment $(-Q^2_{max}, 0)$ transforms to $(-z_{max}, z_{max})$

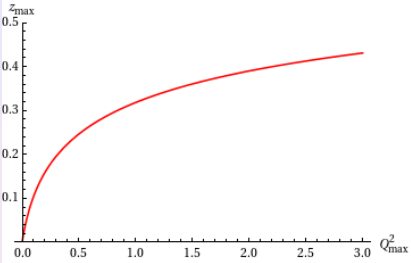

Expansion:

$$G(t) = \sum_{k=0}^{\infty} a_k z^k(t)$$

The main result:
$|a_k|$ can be bounded by the knowledge of the $Im(G)$ in timelike region.

- E-M Form Factors are real on $-q^2 > 0$ line
- $\lim_{|t|\to\infty} |G(t)| \to 0$
-

$$G_E^p(t) = \frac{1}{\pi}\int_{4m_\pi^2}^{\infty} dz \frac{ImG_E^p(z)}{z-t}$$

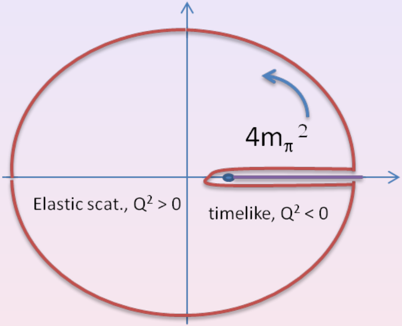

Form-Factors: Time-like-Region

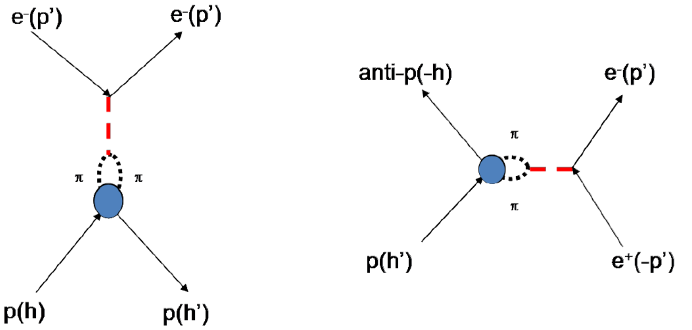

$t=(p-p')^2=(h'-h)^2<0$

$t=(p+p')^2=(h'+h)^2>4\,m_\pi^2$

Interesting property:

$$\mathrm{Im}F_{1,2}=\frac{p_t^3}{\sqrt{t}}\Gamma^*_{1,2}(t) \tag{125}$$

p_t pion momentum in the crossed $(t-)$channel, $\Gamma_{1,2}$ – P-amplitudes for the $\pi\pi - N\overline{N}$.

- Points just above the cut project onto the upper half of the circle (with unit radius)!
- $z(x) = e^{i\theta(t)} \rightarrow$

$$t(\theta) = t_0 + \frac{2(t_{cut} - t_0)}{1 - \cos\theta}$$

- a_k must be Real! Now

$$\mathrm{Re} \int_0^{\pi} d\theta G(t) e^{ik\theta} = \pi a_k$$

Hence

$$\begin{aligned} a_k &= \frac{1}{\pi} \int_0^{\pi} d\theta \mathrm{Re} G(t + i0) \cos(k\theta) \\ &\quad - \frac{1}{\pi} \int_0^{\pi} d\theta Im G(t + i0) \sin(k\theta) \end{aligned}$$

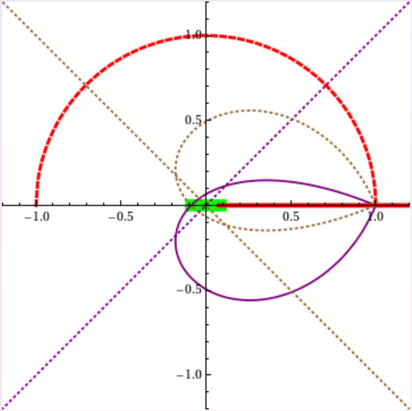

- G(t) is analytic in almost everywhere (cut). Hence $a_{-n} = 0$, for n integer, hence, if one change $k \to -k$ then $\sin$ part is related with $\cos$ part.
-

$$\begin{aligned} a_0 &= G(t_0), \quad z(t_0) = 0. \\ a_{k\geq 1} &= -\frac{2}{\pi}\int_0^{\pi} d\theta ImG[t(\theta)+i0]\sin(k\theta) \\ &= \frac{2}{\pi}\int_{t_{cut}}^{\infty}\frac{dt}{t-t_0}\sqrt{\frac{t_{cut}-t_0}{t-t_{cut}}}ImG(t)\sin(k\theta) \end{aligned}$$

- Norm

$$\parallel G \parallel_p = \left(\sum_{k=0}^{\infty} |a_k|^p \right)^{1/p}$$

In the case of $p = 2$,

$$\begin{aligned} (\parallel G \parallel_2)^2 &= \sum_{k=0}^{\infty} |a_k|^2 = \int_0^{\pi} d\theta G(z) G^*(z) = \int_0^{\pi} d\theta |G(z)|^2 = \oint \frac{dz}{z} |G(z)|^2 \\ &= \frac{1}{\pi} \int_{t_{cut}}^{\infty} \frac{dt}{t - t_0} \sqrt{\frac{t_{cut} - t_0}{t - t_{cut}}} |G(t)^2| \end{aligned}$$

$$\int_0^{\pi} d\theta \, (z^k a_k + z^n a_n)(z^{*k} a_k + z^{*n} a_n) = \int_0^{\pi} d\theta \, (2\cos[(n-k)\theta]) a_k a_n + \pi (a_k^2 + a_n^2) \quad (2)$$

Below two nucleon production

$$F_i^{(I=0)} \sim \frac{\alpha_i m_\omega^2}{m_\omega^2 - t - i\Gamma_\omega m_\omega},$$
$$F_i^{(I=1)} \sim \frac{\beta_i m_\rho^2}{m_\rho^2 - t - i\Gamma_\rho m_\rho}, \quad (19)$$

with $\alpha_1 \approx 1$, $\alpha_2 \approx -0.12$, $m_\omega = 783$ MeV, $\Gamma_\omega = 8.5$ MeV for the isoscalar channel; and $\beta_1 \approx 1$, $\beta_2 \approx 3.7$, $m_\rho = 775$ MeV, $\Gamma_\rho = 149$ MeV for the isovector channel. At $\Gamma = 0$, the ansatz is normalized to the $t = 0$ values in Sec. III A.

TABLE II. Typical bounds on the coefficient ratios $\sqrt{\sum_k a_k^2/a_0^2}$ (upper part of table) and $|a_k/a_0|$ (lower part) in a vector dominance ansatz. ϕ_{OPE} is defined in Eq. (23).

		$t_0 = 0$	$t_0 = t_0^{\mathrm{opt}}$ (0.5 GeV^2)
$\phi = 1$	$\lVert G_E^{(0)} \rVert_2 / G_E^{(0)}(t_0)$	7.6	12.1
	$\lVert G_E^{(1)} \rVert_2 / G_E^{(1)}(t_0)$	2.5	3.9
$\phi = \phi_{\mathrm{OPE}}$	$\lVert \phi^{(0)} G_E^{(0)} \rVert_2 / \phi^{(0)}(t_0) G_E^{(0)}(t_0)$	14.4	23.5
	$\lVert \phi^{(1)} G_E^{(1)} \rVert_2 / \phi^{(1)}(t_0) G_E^{(1)}(t_0)$	4.6	6.7
$\phi = 1$	$2\sqrt{\frac{t_{\mathrm{cut}} - t_0}{m_V^2 - t_{\mathrm{cut}}}}\Big\|_{I=0}$	1.3	1.8
	$2\sqrt{\frac{t_{\mathrm{cut}} - t_0}{m_V^2 - t_{\mathrm{cut}}}}\Big\|_{I=1}$	0.78	1.3

Below two nucleon production

D. Explicit $\pi\pi$ continuum

We can be more explicit in the case of the isovector form-factor expansion, where the leading singularities are due to $\pi\pi$ continuum contributions that are in principle constrained by measured $\pi\pi$ production and $\pi\pi \to N\bar{N}$ annihilation rates [6,23,25]:

$$\mathrm{Im}\, G_E^{(1)}(t) = \frac{2}{m_N\sqrt{t}}(t/4 - m_\pi^2)^{3/2} F_\pi(t)^* f_+^1(t), \qquad (21)$$

where $F_\pi(t)$ is the pion form factor (normalized according to $F_\pi(0) = 1$) and $f_+^1(t)$ is a partial amplitude for $\pi\pi \to N\bar{N}$. Using that these quantities share the same phase [25], we may substitute absolute values. Strictly speaking, this relation holds up to the four-pion threshold, $t \le 16m_\pi^2$. For the purposes of estimating coefficient bounds, we will take the extension of (21) assuming phase equality through the ρ peak as a model for the total $\pi\pi$ continuum contribution.

For $|F_\pi(t)|$ we take an interpolation using the four t values close to production threshold from [26] (0.101 to 0.178 GeV^2), and 43 t values from [27] (0.185 to 0.94 GeV^2). Values for $f_+^1(t)$ are taken from Table 2.4.6.1 of [28]. Evaluating (15) using (21) and the experimental data up to $t = 0.8$ GeV$^2 \approx 40m_\pi^2$ yields for the first few coefficients, at $\phi = 1$ and $t_0 = 0$: $a_0 \approx 2.1$ $a_1 \approx -1.4$, $a_2 \approx -1.6$, $a_3 \approx -0.9$, $a_4 \approx 0.2$. Using $|\sin(k\theta)| \le 1$ in the integral gives $|a_k| \lesssim 2.0$ for $k \ge 1$.

The leading singularities in the isoscalar channel could in principle be analyzed using data for the 3π continuum. Since we do not attempt to raise the isoscalar threshold in our analysis, we content ourselves with a simple vector dominance model to estimate the coefficient bounds. The first few coefficients for the isoscalar form factor using (20) for a narrow ω resonance are: $a_0 = 1$, $a_1 \approx -1.2$, $a_2 \approx -0.96$, $a_3 \approx 0.4$, $a_4 \approx 1.3$. We will compare the above values to those extracted from electron scattering data later. For the moment we note that a bound $|a_k| \le 10$ is conservative.

F. Bounds on the region $t \geq 4m_N^2$

The contribution of the physical region $t \geq 4m_N^2$ to $\|\phi G_E\|_2$ is

$$\delta\|\phi G_E\|_2^2 = \frac{1}{\pi}\int_{4m_N^2}^{\infty} \frac{dt}{t-t_0}\sqrt{\frac{t_{\rm cut}-t_0}{t-t_{\rm cut}}}|\phi G_E|^2. \tag{24}$$

The cross section for $e^+e^- \to N\bar{N}$ is [29]

$$\sigma(t) = \frac{4\pi\alpha^2}{3t}\sqrt{1-\frac{4m_N^2}{t}}\left(|G_M(t)|^2 + \frac{2m_N^2}{t}|G_E(t)|^2\right), \tag{25}$$

and thus for the proton electric form factor we have

$$\delta\|\phi G_E^p\|_2^2 = \frac{1}{\pi}\int_{4m_N^2}^{\infty} \frac{dt}{t-t_0}\sqrt{\frac{t_{\rm cut}-t_0}{t-t_{\rm cut}}}|\phi|^2 \times\left[\frac{\sigma(t)}{\sigma_0(t)v(t)}\frac{1}{|G_M/G_E|^2 + 2m_N^2/t}\right], \tag{26}$$

where $\sigma_0 = 4\pi\alpha^2/3t$ and $v(t) = \sqrt{1-4m_N^2/t}$ is the nucleon velocity in the center-of-mass frame. Using the data from [30] (see also [31,32]), we can perform the integral from $t = 4.0$ GeV^2 to 9.4 GeV^2 assuming $|G_M^p/G_E^p| \lesssim 1$.[7] At $t_0 = 0$ and $\phi = 1$, we find the result $\delta\|G_E^p\|_2^2 \lesssim (0.03)^2$, to be added to the contribution from $t \leq 4m_N^2$. This result is obtained by using for $\sigma(t)$ the measured central value plus

Below two nucleon production

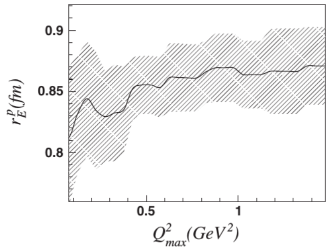

FIG. 3. Variation of the fitted proton charge radius as a function of maximum Q^2. Fits of the proton data were performed with $k_{\max} = 10$, $\phi = 1$, $t_0 = 0$, $|a_k| \leq 10$. Data are from [34].

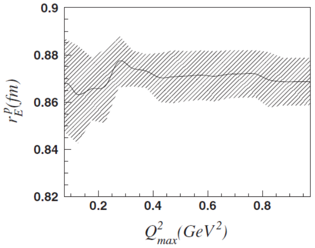

FIG. 4. Variation of the fitted proton charge radius as a function of maximum Q^2. Fits were performed including proton data, neutron data, and the $\pi\pi$ continuum contribution to the isovector spectral function, as detailed in the text. Fits were performed with $k_{\max} = 8$, $\phi = 1$, $t_0 = 0$, $|a_k| \leq 10$.

TABLE III. The rms charge radius extracted using electron-proton and electron-neutron scattering data, and different schemes presented in the text. The neutron form-factor slope is constrained using (31). A cut $Q^2_{\text{max}} = 0.5\ \text{GeV}^2$ is enforced. In the lower part of the table, the bounds on $\sum_k a_k^2$ from Table II are multiplied by 4. ϕ_{VMD} and ϕ_{OPE} are defined in Eqs. (22) and (23).

	$k_{\text{max}} = 2$	3	4	5	6
$\phi = 1,\ t_0 = 0,\ \lvert a_k \rvert \le 10$	888^{+5}_{-5}	865^{+11}_{-11}	888^{+17}_{-22}	882^{+21}_{-22}	878^{+20}_{-19}
	$\chi^2 = 33.67$	23.65	21.80	21.13	20.47
$\phi = 1,\ t_0 = 0,\ \lvert a_k \rvert \le 5$	888^{+5}_{-5}	865^{+11}_{-11}	881^{+10}_{-16}	885^{+16}_{-21}	882^{+18}_{-20}
	$\chi^2 = 33.67$	23.65	21.95	21.46	21.06
$\phi = \phi_{\text{VMD}},\ t_0 = 0,\ \lvert a_k \rvert \le 10$	865^{+6}_{-6}	874^{+12}_{-13}	884^{+23}_{-24}	879^{+24}_{+22}	877^{+22}_{-20}
	$\chi^2 = 23.26$	22.50	22.15	21.59	21.09
$\phi = 1,\ t_0 = 0$	888^{+5}_{-5}	865^{+11}_{-11}	880^{+13}_{-16}	882^{+14}_{-18}	882^{+15}_{-18}
	$\chi^2 = 33.67$	23.65	22.07	21.45	21.18
$\phi = \phi_{\text{OPE}},\ t_0 = 0$	904^{+5}_{-5}	861^{+10}_{-11}	888^{+14}_{-21}	883^{+20}_{-20}	881^{+20}_{-19}
	$\chi^2 = 61.34$	24.38	21.62	20.86	20.51
$\phi = \phi_{\text{OPE}},\ t_0 = t_0^{\text{opt}}(0.5\ \text{GeV}^2)$	912^{+5}_{-5}	869^{+9}_{-9}	887^{+18}_{-19}	881^{+20}_{-19}	880^{+20}_{-19}
	$\chi^2 = 93.69$	22.54	21.05	20.32	20.32

$$F_A^{\rm dipole}(q^2) = \frac{F_A(0)}{[1 - q^2/(m_A^{\rm dipole})^2]^2}, \qquad (2)$$

different experiments have reported values for the so-called axial mass parameter $m_A^{\rm dipole}$. World averages reported by Bernard *et al.* [6] find comparable values obtained from neutrino scattering results prior to 1990, $m_A^{\rm dipole} = 1.026 \pm 0.021$ GeV, and from pion electro-production, $m_A^{\rm dipole} = (1.069 - 0.055) \pm 0.016$ GeV.[1] The NOMAD Collaboration reports [5] $m_A^{\rm dipole} = 1.05 \pm 0.02 \pm 0.06$ GeV. In contrast, MiniBooNE reports [3] $m_A^{\rm dipole} = 1.35 \pm 0.17$ GeV, and other recent results from the K2K SciFi [1], K2K SciBar [7], and MINOS [8]

$$F_P(q^2) \approx \frac{2m_N^2}{m_\pi^2 - q^2} F_A(q^2). \qquad (4)$$

The axial-vector form factor is normalized at $q^2 = 0$ by neutron beta decay (see Table II). Our main focus is on determining the q^2 dependence of $F_A(q^2)$ in the physical region of quasielastic neutrino scattering, $Q^2 = -q^2 \geq 0$. As discussed in the introduction, an expansion at $q^2 = 0$ defines an "axial mass parameter" m_A, via

$$F_A(q^2) = F_A(0)\left[1 + \frac{2}{m_A^2} q^2 + \cdots\right] \Rightarrow m_A \equiv \sqrt{\frac{2F_A(0)}{F_A'(0)}}.$$

The expansion coefficients appearing in (9) can be used to define norms,

$$||F_A||_p = \left(\sum_k |a_k|^p\right)^{1/p}. \quad (12)$$

In particular, $||F_A||_\infty = \sup_k |a_k| = \lim_{p\to\infty} ||F_A||_p$ provides a bound on the maximum coefficient size. The finiteness of the integral appearing in the relation

$$||F_A||_2 = \left(\frac{1}{\pi}\int_{t_{cut}}^{\infty} \frac{dt}{t-t_0}\sqrt{\frac{t_{cut}-t_0}{t-t_{cut}}}|F_A(t)|^2\right)^{1/2}, \quad (13)$$

together with $||F_A||_\infty \le ||F_A||_2$, establishes that a finite upper bound exists for the coefficients. As a first approach to estimating the actual bound $||F_A||_\infty$, consider an "axial-vector dominance" ansatz, $F_A \sim m_{a_1}^2/(m_{a_1}^2 - t - i\Gamma_{a_1} m_{a_1})$, where $m_{a_1} = 1230(40)$ MeV and $\Gamma_{a_1} = 250$–600 MeV are the mass and width of the lowest lying axial-vector, isovector meson [11]. More precisely, let us define the form factor via its dispersion relation with [15]

$$\mathrm{Im}\, F_A(t+i0) = \frac{\mathcal{N} m_{a_1}^3 \Gamma_{a_1}}{(t-m_{a_1}^2)^2 + \Gamma_{a_1}^2 m_{a_1}^2}\theta(t-t_{cut}), \quad (14)$$

Using the dispersion relation (7) with (14) we find

$$F_A(t+i0) = \frac{\mathcal{N}}{\pi}\frac{m_{a_1}^3\Gamma_{a_1}}{|b(t)|^2}\left[\frac{1}{2}\log\left(\frac{|b(t_{cut})|^2}{|t_{cut}-t|^2}\right) + \frac{m_{a_1}^2 - t}{m_{a_1}\Gamma_{a_1}}\arg[b(t_{cut})] + i\pi\theta(t-t_{cut})\right], \quad (15)$$

where $b(t) = t - m_{a_1}^2 + i\Gamma_{a_1} m_{a_1}$, and $\mathcal{N}$ is determined by the value of $F_A(0)$. Table I displays the values for $||F_A||_2$ and $||F_A||_\infty$ computed in this ansatz. For the latter quantity one can show that

$$\left|\frac{a_k}{a_0}\right| \le \frac{2|\mathcal{N}|}{|F_A(t_0)|}\,\mathrm{Im}\left(\frac{-m_{a_1}^2}{b(t_{cut}) + \sqrt{(t_{cut}-t_0)b(t_{cut})}}\right). \quad (16)$$

PHYSICAL REVIEW D **84,** 073006 (2011)

TABLE I. Typical bounds on the coefficient ratios $\sqrt{\sum_k a_k^2/a_0^2}$ (first line of table) and $|a_k/a_0|$ (second line) in an axial-vector dominance ansatz. The range corresponds to the range 250–600 MeV for the a_1 width and the range 1190–1270 MeV for the a_1 mass.

	$t_0 = 0$	$t_0 = t_0^{opt}(1.0\ \mathrm{GeV}^2)$
$\|\|F_A\|\|_2/\|F_A(t_0)\|$	1.5–1.7	1.9–2.3
$\|\|F_A\|\|_\infty/\|F_A(t_0)\|$	1.0–1.4	1.4–1.8

PHYSICAL REVIEW D **84**, 073006 (2011)

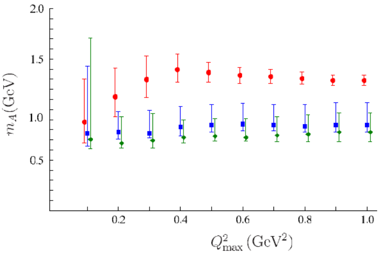

FIG. 2 (color online). Extracted value of m_A versus $Q^2_{\rm max}$. Dipole model results for $m_A^{\rm dipole}$ are shown by the red circles; z expansion results with $|a_k| \leq 5$ are shown by the blue squares, z expansion results with $|a_k| \leq 10$ are shown by the green diamonds.

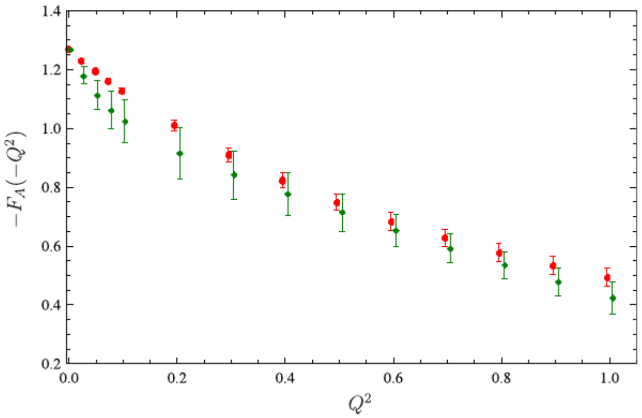

FIG. 3 (color online). Comparison of the axial-vector form factor F_A as extracted using the z expansion (green diamonds) and dipole ansatz (red circles)

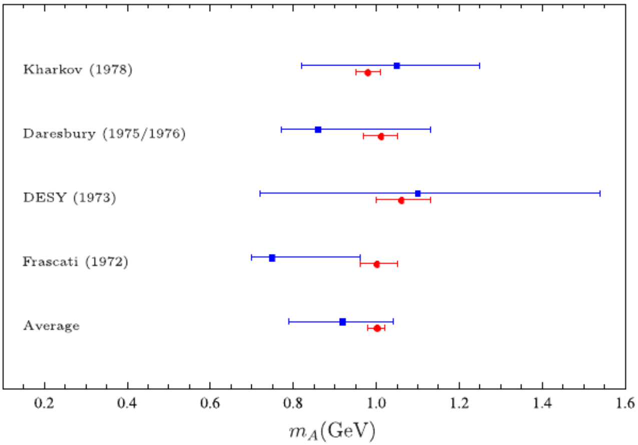

FIG. 4 (color online). Extraction of m_A using charged-pion electroproduction measurements, in the dipole ansatz and in the z expansion. Data sets are as described in the text. Dipole results are shown as the red circles, and z expansion results with $|a_k| \leq 5$ are shown as the blue squares.

$$r_A = \begin{cases} 0.80^{+0.07}_{-0.17} \pm 0.12 \text{ fm} & \text{(neutrino scattering)} \\ 0.74^{+0.12}_{-0.09} \pm 0.05 \text{ fm} & \text{(electroproduction)} \end{cases} . \quad (24)$$

K. M. Graczyk, C. Juszczak, arXiv:1408.0150

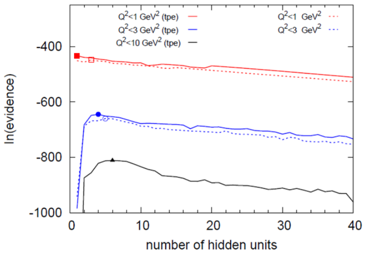

FIG. 2: (Color online) Logarithm of evidence for the best neural networks in each scheme. Solid/dashed lines correspond to the analyses of the data corrected/not corrected by the TPE effect. Points mark the best models for each analysis.

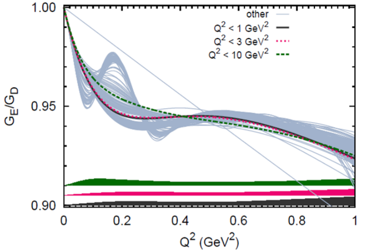

FIG. 3: (Color online) The form factor G_E/G_D ($G_D = 1/(1+Q^2/0.71\mathrm{GeV}^2)^2$). Red, blue and magenta lines correspond to the best models in the analysis with data limited by $Q^2_{\mathrm{cutoff}} = 1, 3$ and $10\ \mathrm{GeV}^2$ respectively. The areas colored with magenta, blue and red denote 1σ uncertainty due to the change in the fit parameters (calculated within the Hessian approximation). The gray lines show models which are best for neural networks with definite number of hidden units, but are not globally best.

proved to obtain the two-photon exchange (TPE) correction to unpolarized elastic ep cross section. However, because of some physical assumptions these analyses were

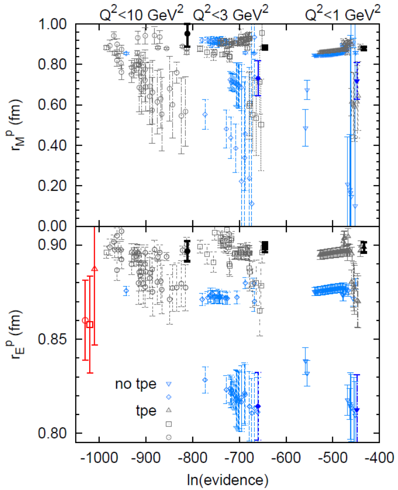

FIG. 4: (Color online) The proton radii corresponding to the models which are the best within particular data selection and neural network scheme. The results for the data corrected by the TPE are marked with black △, □, and ◯ for $Q^2_{\rm cutoff} = 1$, 3 and 10 GeV^2 respectively. The results for the uncorrected data are marked with blue ∇ and ◊ for $Q^2_{\rm cutoff} = 1$ and 3 GeV^2 respectively. The filled points mark the best result for each case. The three leftmost red points are the best results according to the minimum of the error function. For clarity their x-coordinate has been changed. Their ln(evidence) val-

Q^2_{cutoff} (GeV^2)	r^p_M (fm)	r^p_E (fm)	H
1	0.879 ± 0.007	0.899 ± 0.003	1
3	0.883 ± 0.007	0.899 ± 0.003	4
10	0.953 ± 0.065	0.897 ± 0.005	6

TABLE I: The values of the proton radii obtained with 1σ uncertainty due to variation in the parameter space. H is the number of hidden units of the best model.

Q^2_{cutoff} (GeV^2)	r^p_M (fm)	r^p_E (fm)
1	0.8792 ± 0.0006	0.8989 ± 0.0001
3	0.8828 ± 0.0063	0.8988 ± 0.0003
10	0.9205 ± 0.0606	0.8968 ± 0.0029

TABLE II: The expected value (according to evidence probability distribution) of the proton radii with systematic uncertainty due to the choice of the parametrization (given by the variance).

Bjorken, J., & Drell, S. D. (1998). *Relativistic quantum mechanics*. McGraw-Hill Education.